Room temperature DBR-free VCSEL operation on InGaN/GaN thin film platform with monolithic surface grating

WAI YUEN FU[1], ZHONGQI WANG[1], YUK FAI CHEUNG[1], AND HOI WAI CHOI[*]

[1] *Department of Electrical and Electronic Engineering, the University of Hong Kong, Pokfulam Road, Hong Kong*
[*] *hwchoi@hku.hk*

Received 2 July 2024; revised 20 July 2024; accepted 25 July 2024; posted 25 July 2024; published 2 August 2024

Vertical-cavity surface-emitting lasers (VCSELs) are pivotal in various applications ranging from data communication to sensing technologies. This study introduces a VCSEL design featuring a monolithic top surface high contrast grating (HCG) reflector on a thin film substrate, aimed at improving lasing performance while reducing fabrication costs by omitting the use of Distributed Bragg Reflectors (DBRs). We fabricated the proposed VCSEL with the surface grating and characterized its performance through micro-photoluminescence measurements. The laser demonstrated room temperature lasing at 436.2 nm with a Q factor of 4600 and a lasing threshold of 5.5 kW/cm^2 under optical pumping. The implementation of the surface grating reflector was instrumental in facilitating vertical lasing, significantly improving surface reflectivity compared to conventional flat GaN/air interfaces. This innovative design holds significant promise for the development of cost-effective, DBR-free VCSELs, with potential applications extending to photonic integrated circuits and LiDAR systems.

https://doi.org/10.1364/OL.534465

Visible light Indium Gallium Nitride (InGaN) based lasers have become pivotal in the field of optoelectronics [1], providing significant benefits for applications such as optical storage (Blu-ray), laser display technology, and visible light communication. Conventionally, research on InGaN-based lasers has focused on vertical-cavity surface-emitting lasers (VCSELs) and edge-emitting lasers [2–4], but interest in InGaN microdisk lasers is growing, particularly with their successful demonstration of lasing under electrical injection [5–13]. The integration of thin film technology has proven especially advantageous in this context [13]. Traditional laser diodes, utilize pairs of Distributed Bragg Reflectors (DBRs) [14–20] or waveguiding layers [21], grown inside the epitaxy to form laser cavities — a process that can be cost-intensive. In contrast, thin film technology employs a conventional LED film that is eutectic bonded to a foreign substrate with a reflective metallic layer [22], followed by thinning to an optimized thickness [7], thus enhancing the optical confinement and overlap factor [23], leading to a substantial increase in laser quality (Q) factor [8].

The successful demonstration of thin film technology in enhancing the Q factor of microdisk lasers under electrical injection, as detailed in our previous papers [7, 8, 13], underscores its potential for implementation in various InGaN laser devices. While the bottom thin film surface is optically confined with a metallic reflective layer, the top GaN/air interface presents an opportunity for further enhancement. Although depositing a costly DBR on the top surface could improve optical confinement, the unique structure of the thin film invites an alternative approach—using a nanostructured surface to enhance top surface reflectivity.

Thus this report introduces a method to implement a VCSEL without DBR by incorporating a surface high contrast grating (HCG) monolithically as a top reflector for the lasing cavity, significantly boosting reflectivity beyond the flat GaN/air interface on a thin film platform. Previous work by J. Lee et al. [24] demonstrated near-100% broadband reflectivity enhancement through surface grating reflectors. In our study, we have deliberately designed the grating to enhance reflectivity in a narrow band to suppress mode competition. To showcase the effectiveness of the fabricated grating reflector, we refrained from any geometric shaping of the laser cavity, thus relying solely on the newly implemented top surface grating reflector and the existing bottom metallic reflecting layer without any DBR, using the thin film GaN platform.

The introduction of the surface grating reflector not only boosts overall lasing efficiency by enhancing top surface reflectivity but also simplifies implementation, making it adaptable across various laser device configurations that require enhanced top surface reflectivity or tailored light emission redirection. This development promises significant enhancements in the applicability of GaN lasers across a wide range of technological applications, from high-resolution displays to sophisticated communication systems.

The construction of the thin film grating surface-emitting laser begins with an InGaN LED wafer that emits light at a wavelength of 440 nm. This wafer, procured from Enkris Semiconductor Inc, was grown on a silicon substrate through metalorganic chemical vapor deposition (MOCVD). The wafer features a structure that includes multiple quantum wells (MQWs), consisting of 6 pairs of InGaN/GaN

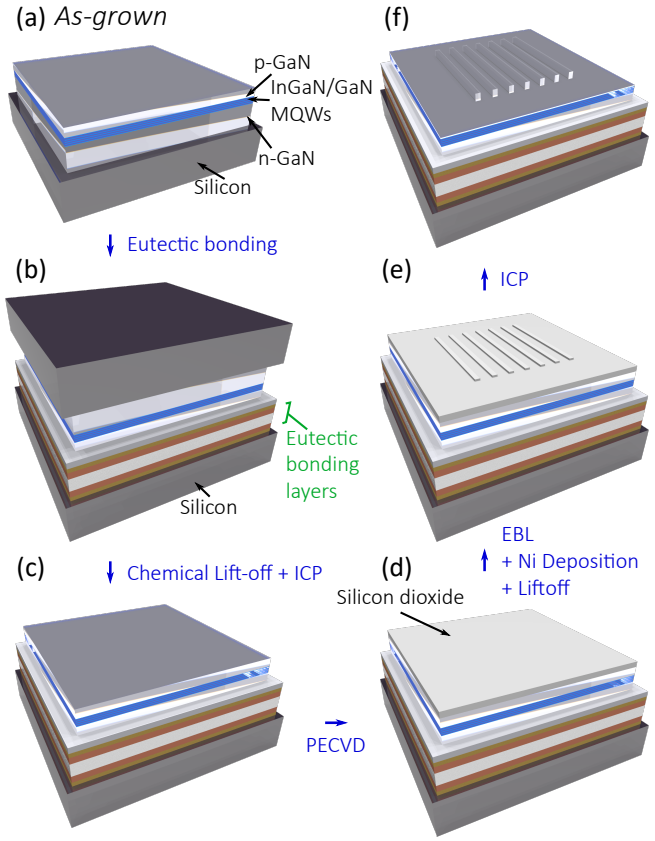

Fig. 1. 3D Schematics of the process flow: (a) as-grown; (b) as-grown wafer eutectic bonded to a Si substrate; (c) Original silicon substrate removed by chemical lift-off followed by thin down by ICP; (d) Oxide deposition by PECVD; (e) EBL of grating pattern, Ni deposition followed by lift-off; (f) ICP etch to fabricate grating.

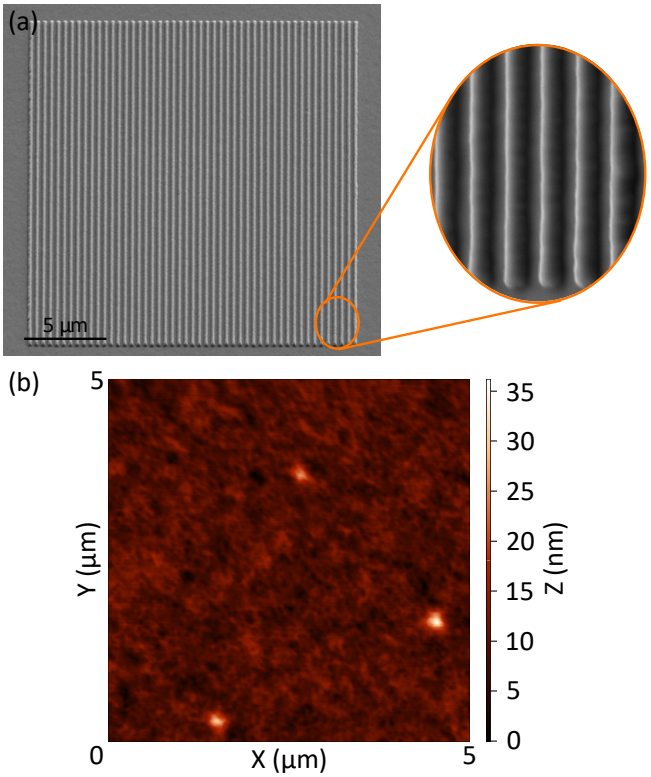

Fig. 2. (a) SEM images of the fabricated grating, with the circular inset showing a zoomed-in SEM image. (b) shows an AFM image of the top n-GaN surface after ICP etch.

quantum wells with respective thicknesses of 5.9 nm and 7.0 nm, respectively. A 200 nm-thick p-GaN layer layer caps the structure.

Fig. 1 illustrates the process flow for fabrication of the thin film VCSEL with top surface grating. Initially, a reflective metal layer composed of Ni/Ag/Ni/Au (5 nm/100 nm/25 nm/50 nm) is deposited onto the top p-GaN surface using electron beam deposition. This is followed by the deposition of a Ti/Au (30 nm/100 nm) metal layer on both the LED wafer (above the p-GaN layer) and the target Si substrate. Subsequently, a Cu/Sn bonding layer is electroplated onto these surfaces. By pressing the LED wafer and the silicon substrate together, with the interposed Cu/Sn bonding layers, and applying high pressure and temperature, a robust eutectic bond is achieved. The original silicon substrate is then detached via a chemical lift-off (CLO) process employing hydrofluoric (HF) acid [22, 23]. The sample subsequently undergoes an inductive coupled plasma (ICP) etch to thin the film to a thickness optimized for resonant cavity formation, during which the buffer layer and u-GaN layer are removed.

The grating fabrication process commences on the prepared thin film sample by initially depositing a silicon dioxide layer via plasma-enhanced chemical vapor deposition (PECVD). Subsequently, the grating pattern is precisely inscribed on this oxide layer using electron beam lithography. Following this patterning step, a 30 nm-thick nickel (Ni) layer is deposited onto the oxide-coated surface. This is followed by a lift-off process to remove excess Ni, thereby ensuring that the grating pattern is accurately transferred first to the oxide layer and subsequently into the underlying GaN layer through an inductive coupled plasma (ICP) etching process. Fig. 2(a) presents Scanning Electron Microscope (SEM) images captured using a Zeiss Sigma 300 VP Field Emission Gun (FEG) Scanning Electron Microscope, which illustrate the detailed grating structure spanning a 20 μm × 20 μm area. Notably, no additional lateral isolation was performed on the VCSEL to suppress side resonances. This intentional design choice serves a specific proof-of-concept purpose, ensuring that the lasing emission is strictly surface-emitting. Fig. 2(b) shows an atomic force microscope (AFM) image of the top n-GaN surface following the fabrication process, taken using an NT-MDT NTEGRA AFM. It illustrates that the surface remains optically smooth, exhibiting an RMS roughness of 2.26 nm.

Prior to initiating the fabrication process, the grating pattern undergoes simulation using finite element method (FEM) software, COMSOL. As a one-dimensional (1D) photonic structure, the grating on the epitaxial layer is modeled through a two-dimensional (2D) FEM simulation, incorporating periodic boundary conditions on both the +x and -x sides of the simulation region to emulate an infinite periodic structure. The optimization of the grating reflector's reflectivity is constrained by fabrication limitations. Considering the etch selectivity, a grating height of 250 nm is selected, supported by a Ni mask thickness of 30 nm. After thorough simulations, a grating period of approximately 360 nm is chosen, tailored to achieve maximal reflectivity.

As depicted in Fig. 3(a), the simulated reflection spectrum of the surface grating with a period of 360 nm and a duty cycle of 0.45 exhibit narrowband reflection peaks that achieve up to 100% reflectivity under normal incidence from within the GaN medium. The simulation reveals five reflectance peaks: three broader peaks at wavelengths 407.1 nm, 428.5 nm, and 448.9 nm correspond to vertical confinement modes, which are crucial for VCSEL operation, while the two narrower peaks at 416.4 nm and 424.9 nm represent waveguiding modes that primarily

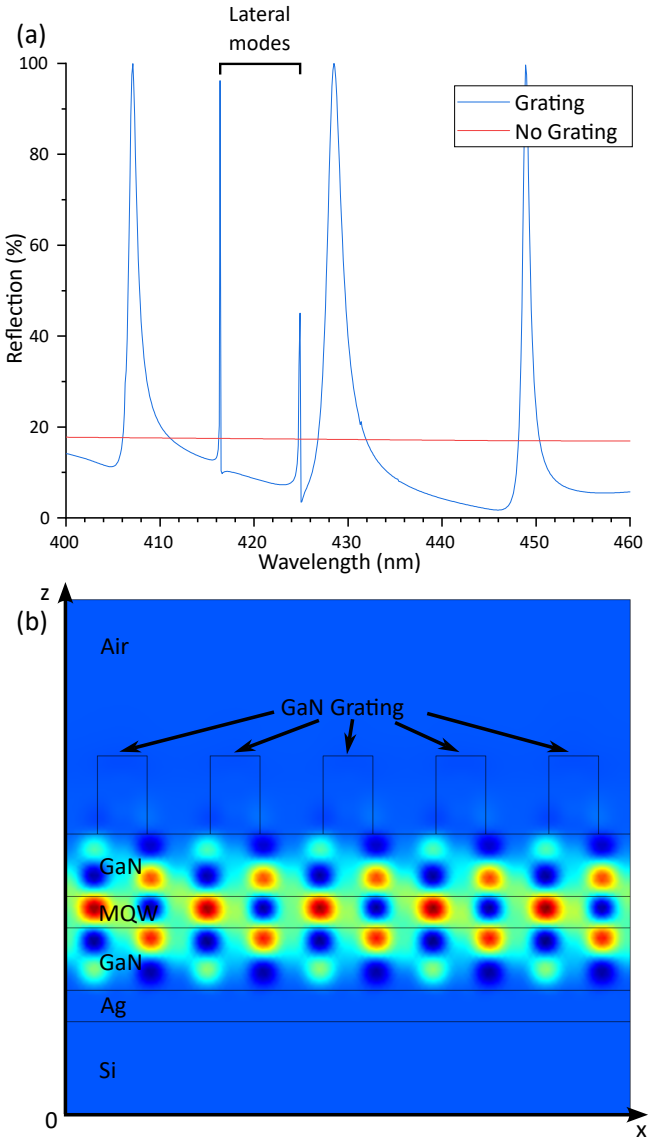

Fig. 3. (a) Reflection spectra under normal incidence from within the GaN medium; and (b) electric field profile, simulated by finite-element analysis.

propagate laterally. These lateral modes appear in the simulation due to the implementation of periodic boundary conditions, and are not anticipated to occur in the actual device. Importantly, the separation between these broader peaks is sufficiently large, ensuring that only one reflection peak coincides with the luminescence spectrum of the MQWs. This strategic peak placement is crucial for suppressing mode competition, potentially lowering the lasing threshold and enhancing the Q factor. For comparative purposes, the reflectivity of GaN without the grating is also simulated and illustrated in Fig 3(a). This reflectivity profile is basically flat and shows a lower reflectivity at around 17.8%, underscoring the significant improvement offered by the grating structure.

Fig. 3(b) demonstrates the electric field profile of the complete VCSEL structure with the top surface grating under resonant conditions. The cavity length, defined as the distance between the bottom metallic layer and the top surface grating, is optimized to approximately 500 nm. This adjustment ensures that the main resonance node is precisely aligned with the active region where the MQWs are located, as illustrated by Fig. 3(b). From the 2D FEM calculations, a Q factor of approximately 73000 is estimated at the 432 nm reflection peak, demonstrating the effectiveness of the surface grating design in enhancing lasing performance.

Following the fabrication of the grating structure on the thin film sample, micro-photoluminescence (μ-PL) measurements were conducted to characterize the lasing characteristics. A CNI pulsed laser, TUN-TiA-393-408, emitting at 393.32 nm with a pulse width of 29.25 ns and a repetition rate of 50 kHz, was employed for optical pumping of the fabricated VCSEL. The emitted free-space PL signals were collected and directed into a Horiba iHR 550 spectrograph, equipped with a Syncerity BI UV-Vis deep-cooled CCD. This setup provided an effective optical resolution of 0.024 nm using a 2400 g/mm grating.

The measured μ-PL spectra are shown in Fig. 4(a). The lasing peak is at around 436.2 nm which is a fairly good match with the simulated resonance peak of 432 nm shown in Fig. 3. The minor discrepancy may arise from the use of 2D simulation instead of 3D. The corresponding linewidth vs excitation power density plot is shown in Fig. 4(b), illustrating a lasing threshold of around 5.5 kW/cm^2 and a Q factor of 4600. In contrast, areas lacking the grating structure showed no lasing emissions, even when the excitation power was ramped up to approximately 30 kW/cm^2, at which point the beam began damaging the sample. This observation suggests that lateral resonance modes are effectively suppressed in the absence of geometrical configurations such as microdisks or edge-emitting cavities. Moreover, it is evident that the surface grating significantly enhances the surface reflectivity of the thin film sample, thereby facilitating lasing in the vertical direction. The inset in Fig. 4(b)displays the reflection spectra of the bottom metallic reflector and the high contrast grating (HCG) structure, measured from the top side under normal incidence using an Ocean Optics HL-2000 halogen light source and an Ocean Insight STAN-SSH as a specular reflectance standard. Notably, the reflection peak of the HCG now appears as a dip, a result of the measurement being conducted from the top side, contrary to the design and simulation that consider emission from within the GaN medium. The broader width observed can similarly be attributed to the use of 2D simulation with periodic boundary conditions, as compared to the actual 3D device with a limited number of grating pairs.

The monolithic surface grating reflector, integrated onto a thin film platform, offers a cost-effective alternative to more expensive enhancements such as DBRs or absorptive metallic layers for improving surface reflectivity. Although the demonstrated lasing threshold of 5.5 kW/cm^2 marks an improvement over earlier studies on InGaN-based VCSELs, which reported thresholds exceeding 100 kW/cm^2 [16, 25], it understandably does not yet match the performance of state-of-the-art VCSELs equipped with refined DBRs that typically lase at well below 100 W/cm^2 [15]. However, the successful demonstration of room-temperature lasing under optical pumping conditions confirms the feasibility of VCSEL operation without DBRs, providing a low-cost solution for lasing devices. This economical VCSEL approach, enabled by the monolithic surface grating reflector and amenable to further threshold reduction through optimization, offers a practical option for applications such as Light Detection and Ranging (LiDAR).

In summary, this study presents a DBR-free VCSEL that incorporates a monolithic top HCG reflector, developed on a thin film platform. Experimental results confirm the efficacy of the surface grating reflector in enabling room temperature lasing at 436.2 nm. Notably, the device achieves a Q factor of 4600 and a lasing threshold of 5.5 kW/cm^2, which closely corresponds with the predictions made by 2D finite element method (FEM) simulations. The successful implementation of VCSEL operation in these DBR-free devices heralds a low-cost

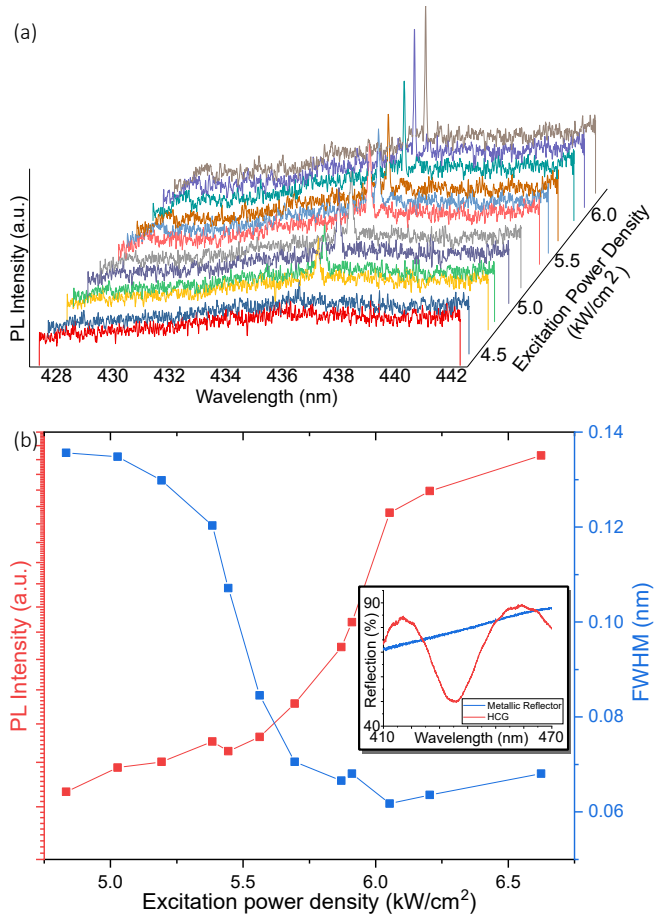

Fig. 4. (a) Room-temperature μ-PL spectra (in linear scale) for thin-film VCSEL with top surface grating under increasing excitation power density; (b) shows the corresponding plots displaying linewidths (in linear scale) in blue and integrated PL intensities (in log scale) in red with increasing excitation power densities. The inset shows the reflection spectra of the bottom metallic reflector and the HCG, as measured under normal incidence from the top side.

approach to laser technologies.

Funding. This work was supported by a General Research Fund (Project 17206922 and Project 17205619), sponsored by the Research Grant Council of Hong Kong SAR.

Disclosures. The authors declare that they have no conflict of interest.

Data Availability Statement. Data underlying the results presented in this paper are not publicly available at this time but may be obtained from the authors upon reasonable request.

REFERENCES

1. S. Nakamura, Annu. Rev. Mater. Res. **28**, 125 (1998).
2. A. Liu, P. Wolf, J. A. Lott, and D. Bimberg, Photonics Res. **7**, 121 (2019).
3. K. H. Li, W. Y. Fu, and H. W. Choi, Prog. Quantum Electron. **70**, 100247 (2020).
4. J. A. Holguin-Lerma, M. Kong, O. Alkhazragi, *et al.*, Opt. Lett. **45**, 742 (2020).
5. M. Feng, J. He, Q. Sun, *et al.*, Opt. Express **26**, 5043 (2018).
6. J. Wang, M. Feng, R. Zhou, *et al.*, Opt. Express **28**, 12201 (2020).
7. K. H. Li, Y. F. Cheung, W. Y. Fu, and H. W. Choi, Appl. Phys. Lett. **119**, 101106 (2021).
8. W. Y. Fu, Y. F. Cheung, and H. W. Choi, Laser & Photonics Rev. **n/a**, 2400047 (2024).
9. J. Wang, M. Feng, R. Zhou, *et al.*, Appl. Phys. Express **13**, 074002 (2020).
10. Y. Tang, M. Feng, H. Zhao, *et al.*, Opt. Express **30**, 13039 (2022).
11. M. Feng, H. Zhao, R. Zhou, *et al.*, ACS Photonics **10**, 2208 (2023).
12. H. Zhao, M. Feng, J. Liu, *et al.*, Opt. Express **31**, 20212 (2023).
13. W. Y. Fu and H. W. Choi, Prog. Quantum Electron. **95**, 100516 (2024).
14. A. Haglund, E. Hashemi, J. Bengtsson, *et al.*, *Progress and challenges in electrically pumped GaN-based VCSELs*, vol. 9892 of *SPIE Photonics Europe* (SPIE, 2016).
15. H.-c. Yu, Z.-w. Zheng, Y. Mei, *et al.*, Prog. Quantum Electron. **57**, 1 (2018).
16. I. L. Krestnikov, W. V. Lundin, A. V. Sakharov, *et al.*, Appl. Phys. Lett. **75**, 1192 (1999).
17. T. Tawara, H. Gotoh, T. Akasaka, *et al.*, Appl. Phys. Lett. **83**, 830 (2003).
18. E. Feltin, G. Christmann, J. Dorsaz, *et al.*, "Blue lasing at room temperature in an optically pumped lattice-matched AlInN/GaN VCSEL structure," (2007).
19. T. Takeuchi, S. Kamiyama, M. Iwaya, and I. Akasaki, Reports on Prog. Phys. **82**, 012502 (2019).
20. K. Terao, H. Nagai, D. Morita, *et al.*, *Blue and green GaN-based vertical-cavity surface-emitting lasers with AlInN/GaN DBR*, vol. 11686 of *SPIE OPTO* (SPIE, 2021).
21. Y. Sun, K. Zhou, M. Feng, *et al.*, Light. Sci. & Appl. **7**, 13 (2018).
22. Y. F. Cheung, K. H. Li, and H. W. Choi, ACS Appl. Mater. & Interfaces **8**, 21440 (2016).
23. W. Y. Fu and H. W. Choi, J. Appl. Phys. **132**, 060903 (2022).
24. J. Lee, S. Ahn, H. Chang, *et al.*, Opt. Express **17**, 22535 (2009).
25. S.-H. Park, J. Kim, H. Jeon, *et al.*, Appl. Phys. Lett. **83**, 2121 (2003).